Structural Engineering and Mechanics, *Vol. 52, No. 1 (2014) 1-17*
DOI: http://dx.doi.org/10.12989/sem.2014.52.1.001

A penny-shaped interfacial crack between piezoelectric layer and elastic half-space

J.H. Ren[a], Y.S. Li[*] and W. Wang[a]

College of Mechanical and Electrical Engineering, Hebei University of Engineering, Handan 056038, P.R. China

(Received January 1, 2013, Revised April 22, 2014, Accepted April 28, 2014)

Abstract. An interfacial penny-shaped crack between piezoelectric layer and elastic half-space subjected to mechanical and electric loads is investigated. Using Hankel transform technique, the mixed boundary value problem is reduced to a system of singular integral equations. The integral equations are further reduced to a system of algebraic equations with the aid of Jacobi polynomials. The stress intensity factor and energy release rate are determined. Numerical results reveal the effects of electric loadings and material parameters of composite on crack propagation and growth. The results seem useful for design of the piezoelectric composite structures and devices of high performance.

Keywords: interfacial crack; penny-shaped crack; Hankel transform; energy release rate; piezoelectric material

1. Introduction

Piezoelectric materials have wide applications in transducers, sensors and actuators due to the electric and mechanical coupling characteristics. Because of the brittle nature, the fracture of piezoelectric materials has received much attention.

The paper of Zhang *et al*. (2002), Zhang and Gao (2004), Kuna (2010) provided extensive reviewing for the current state of the fracture mechanics research of piezoelectric materials. On the penny-shaped crack problems, using the method of potential functions, Wang (1994) obtained the general solution of three-dimensional problems for transversely isotropic piezoelectric materials and analyze the mechanical-electric coupling behavior of penny-shaped crack. Kogan *et al*. (1996) obtained the closed form solution for the penny-shaped crack in an infinite piezoelectric media using harmonic functions. The problem of a penny-shaped crack in a transversely isotropic piezoelectric material loaded by both normal and tangential tractions and by electric charges was analyzed by Karapetian *et al*. (2000). Chen and shioya (2000) presented an exact analysis of the problem of a penny-shaped crack in a transversely isotropic piezoelectric medium subjected to arbitrary shear loading that is antisymmetric with respect to the crack plane. The effect of a penny-shaped crack on the deformation of an infinite piezoelectric material subjected to mode I

∗Corresponding author, Associate Professor, E-mail: liyshbue@163.com
[a]Associate Professor

http://www.techno-press.org/?journal=sem&subpage=8 ISSN: 1225-4568 (Print), 1598-6217 (Online)

electrical and mechanical loading has been studied by Yang (2004) using the theory of linear piezoelectricity and applying appropriate boundary conditions. Yang and Lee (2003a, b) investigated the problems of a penny-shaped crack in a piezoelectric cylinder and in a piezoelectric cylinder surrounded by an elastic medium, respectively. Wang *et al*. (2001) analyzed the problem of a penny-shaped crack in a piezoelectric medium of finite thickness. Li and Lee (2004) investigated the effects of electrical load on crack growth of penny-shaped dielectric cracks in a piezoelectric layer. Feng *et al*. (2006) considered the dynamic fracture behaviors of a penny-shaped crack in a piezoelectric layer. Using the finite element method, three-dimensional cracks of different geometry were considered by Shang *et al*. (2003). Wang *et al*. (2011) studies a penny-shaped crack in a finite thickness piezoelectric material layer which is subjected to a thermal flux on its top and bottom surfaces. Ueda and Ashida (2007), Ueda (2008) investigated the penny-shaped crack in a functionally graded piezoelectric strip.

As far as the interfacial penny-shaped crack problem is considered, an integral equation formulation is successfully developed to analyze the case of a penny-shaped crack at the interface of a piezoelectric bi-material system by Tian and Rajapakse (2006). To the authors' knowledge, the interfacial penny-shaped crack between piezoelectric layer and elastic half space subjected to electroelastic loadings has not been considered.

The objective of this paper is to seek the solution to the interfacial penny-shaped crack problem between piezoelectric layer and elastic half-space. This is a two-dimension axisymmetric problem. A system of algebraic equations is derived using the Hankel transform and Cauchy singular integral equation methods. The stress intensity factor (SIF) and energy release rate (ERR) of crack tip are obtained and numerically solved. It is shown that the crack tip behaviors depend strongly upon the electric loadings, material parameters of composite, which could be of particular interest to the analysis and design of smart sensors/actuators constructed from piezoelectric composite laminates.

2. Basic formulations

As shown in Fig. 1, a penny-shaped crack with the radius a perpendicular to the poling axis is situated at the interface of piezoelectric layer and elastic half sapce and occupies the region $0 \le r < a$, $z=0$. The thickness of piezoelectric layer is h.

The boundary conditions for the penny-shaped crack problem are set as

$$\sigma_{rz}(r,0)=\sigma_{rz}^E(r,0)=0,\ \sigma_{zz}(r,0)=\sigma_{zz}^E(r,0)=0,\ D_z(r,0)=0,\ (0\le r<a) \tag{1a}$$

$$\sigma_{rz}(r,0)=\sigma_{rz}^E(r,0),\ \sigma_{zz}(r,0)=\sigma_{zz}^E(r,0),\ D_z(r,0)=0,\ (a\le r<\infty) \tag{1b}$$

$$u_r(r,0)=u_r^E(r,0),\ u_z(r,0)=u_z^E(r,0),\ (a\le r<\infty) \tag{1c}$$

$$\sigma_{rz}(r,h)=p_1(r),\ \sigma_{zz}(r,h)=p_2(r),\ (0\le r<\infty) \tag{1d}$$

$$D_z(r,h)=p_3(r),\ (0\le r<\infty) \tag{1e}$$

where σ_{rz}, σ_{zz} and D_z are stresses and electric displacement of the piezoelectric layer; σ_{rz}^E and σ_{zz}^E are stresses components of the elastic half-space; u_r and uz_r are the displacement components of

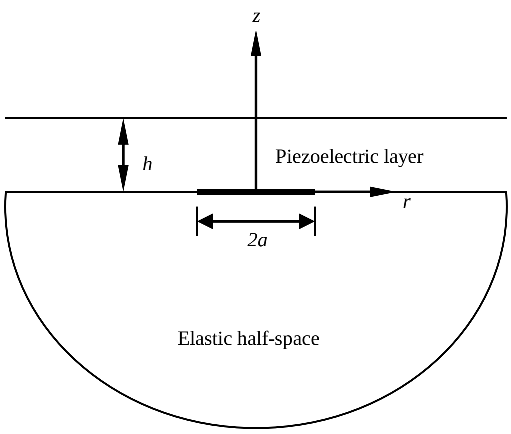

Fig. 1 Configuration of the interfacial penny-shaped crack problem

the piezoelectric layer; u_r^E and u_z^E are the displacement components of the elastic half-space; $p_1(r)$, $p_2(r)$ and $p_3(r)$ are given amplitude of the applied loadings respectively.

2.1 Piezoelectric layer

Consider a transversely isotropic piezoelectric material with a cylindrical polar coordinate system defined with (r, θ, z) as the plane of isotropy and z-axis as the poling direction.

In the case of axisymmetric deformations, the elastic displacement components and the electric potential are functions of only r and z. The constitutive equations can be expressed in terms of the elastic displacements and electric potential as

$$\sigma_{rr} = c_{11}\frac{\partial u_r}{\partial r} + c_{12}\frac{u_r}{r} + c_{13}\frac{\partial u_z}{\partial z} + e_{31}\frac{\partial \phi}{\partial z} \tag{2a}$$

$$\sigma_{\theta\theta} = c_{12}\frac{\partial u_r}{\partial r} + c_{11}\frac{u_r}{r} + c_{13}\frac{\partial u_z}{\partial z} + e_{31}\frac{\partial \phi}{\partial z} \tag{2b}$$

$$\sigma_{zz} = c_{13}\frac{\partial u_r}{\partial r} + c_{13}\frac{u_r}{r} + c_{33}\frac{\partial u_z}{\partial z} + e_{33}\frac{\partial \phi}{\partial z} \tag{2c}$$

$$\sigma_{rz} = c_{44}\left(\frac{\partial u_r}{\partial z} + \frac{\partial u_z}{\partial r}\right) + e_{15}\frac{\partial \phi}{\partial r} \tag{2d}$$

$$D_r = e_{15}\left(\frac{\partial u_r}{\partial z} + \frac{\partial u_z}{\partial r}\right) - \varepsilon_{11}\frac{\partial \phi}{\partial r} \tag{2e}$$

$$D_z = e_{31}\frac{\partial u_r}{\partial r} + e_{31}\frac{u_r}{r} + e_{33}\frac{\partial u_z}{\partial z} - \varepsilon_{33}\frac{\partial \phi}{\partial z} \tag{2f}$$

where ϕ is the electric potential; c_{ij} and e_{ij} (i,j=1,3,4,5) are elastic and piezoelectric constants, respectively; ε_{ij} (i,j=1,3) is dielectric permeablility coefficient.

In the absence of body forces and electric charges, the equilibrium equations can be expressed as

$$c_{11}\left(\frac{\partial^2 u_r}{\partial r^2}+\frac{1}{r}\frac{\partial u_r}{\partial r}-\frac{1}{r^2}\right)+c_{44}\frac{\partial^2 u_r}{\partial z^2}+\left(c_{13}+c_{44}\right)\frac{\partial^2 u_z}{\partial r\partial z}+\left(e_{31}+e_{15}\right)\frac{\partial^2 \phi}{\partial r\partial z}=0 \tag{3a}$$

$$\left(c_{13}+c_{44}\right)\left(\frac{\partial^2 u_r}{\partial r\partial z}+\frac{1}{r}\frac{\partial u_r}{\partial z}\right)+c_{44}\left(\frac{\partial^2 u_z}{\partial r^2}+\frac{1}{r}\frac{\partial u_z}{\partial r}\right)+c_{33}\frac{\partial^2 u_z}{\partial z^2}+e_{15}\left(\frac{\partial^2 \phi}{\partial r^2}+\frac{1}{r}\frac{\partial \phi}{\partial r}\right)+e_{33}\frac{\partial^2 \phi}{\partial z^2}=0 \tag{3b}$$

$$\left(e_{15}+e_{31}\right)\left(\frac{\partial^2 u_r}{\partial r\partial z}+\frac{1}{r}\frac{\partial u_r}{\partial z}\right)+e_{15}\left(\frac{\partial^2 u_z}{\partial r^2}+\frac{1}{r}\frac{\partial u_z}{\partial r}\right)+e_{33}\frac{\partial^2 u_z}{\partial z^2}-\varepsilon_{11}\left(\frac{\partial^2 \phi}{\partial r^2}+\frac{1}{r}\frac{\partial \phi}{\partial r}\right)-\varepsilon_{33}\frac{\partial^2 \phi}{\partial z^2}=0 \tag{3c}$$

The solution to the governing equations can be obtained by means of Hankel transform with respect to the variable r. It can be expressed as

$$u_r\left(r,z\right)=\sum_{j=1}^{6}\int_0^\infty a_{1j}\exp\left(\rho\lambda_{1j}z\right)A_{1j}\left(\rho\right)J_1\left(\rho r\right)d\rho \tag{4a}$$

$$u_z\left(r,z\right)=\sum_{j=1}^{6}\int_0^\infty a_{2j}\exp\left(\rho\lambda_{1j}z\right)A_{1j}\left(\rho\right)J_0\left(\rho r\right)d\rho \tag{4b}$$

$$\phi\left(r,z\right)=\sum_{j=1}^{6}\int_0^\infty a_{3j}\exp\left(\rho\lambda_{1j}z\right)A_{1j}\left(\rho\right)J_0\left(\rho r\right)d\rho \tag{4c}$$

where ρ is the Hankel transform parameter; $A_{1j}(\rho)$(j=1,2,…,6) are unknown functions to be determined and J_i(i=0,1) are i th order Bessel functions of the first kind. The constants {a_{1j}, a_{2j}, a_{3j}} and parameters λ_{1j} are given in Appendix A.

The general solution for relevant components of stress and electric displacement can be expressed as

$$\sigma_{rz}\left(r,z\right)=\sum_{j=1}^{6}\int_0^\infty C_{1j}\exp\left(\rho\lambda_{1j}z\right)A_{1j}\left(\rho\right)J_1\left(\rho r\right)\rho d\rho \tag{5a}$$

$$\sigma_{zz}\left(r,z\right)=\sum_{j=1}^{6}\int_0^\infty C_{2j}\exp\left(\rho\lambda_{1j}z\right)A_{1j}\left(\rho\right)J_0\left(\rho r\right)\rho d\rho \tag{5b}$$

$$D_z\left(r,z\right)=\sum_{j=1}^{6}\int_0^\infty C_{3j}\exp\left(\rho\lambda_{1j}z\right)A_{1j}\left(\rho\right)J_0\left(\rho r\right)\rho d\rho \tag{5c}$$

where C_{1j}, C_{2j} and C_{3j} are also given in Appendix A.

2.2 Elastic half-space

The displacements and stresses in an elastic half-space can be expressed as

$$u_r^E(r,z)=\sum_{j=1}^{2}\int_0^\infty a_{1j}^E \exp\left(\rho\lambda_{2j}z\right)A_{2j}(\rho)J_1(\rho r)d\rho \tag{6a}$$

$$u_z^E(r,z)=\sum_{j=1}^{2}\int_0^\infty a_{2j}^E \exp\left(\rho\lambda_{2j}z\right)A_{2j}(\rho)J_0(\rho r)d\rho \tag{6b}$$

$$\sigma_{rz}^E(r,z)=\sum_{j=1}^{2}\int_0^\infty C_{1j}^E \exp\left(\rho\lambda_{2j}z\right)A_{2j}(\rho)J_1(\rho r)\rho d\rho \tag{6c}$$

$$\sigma_{zz}^E(r,z)=\sum_{j=1}^{2}\int_0^\infty C_{2j}^E \exp\left(\rho\lambda_{2j}z\right)A_{2j}(\rho)J_0(\rho r)\rho d\rho \tag{6d}$$

where $\{a_{1j}^E, a_{2j}^E\}$, $\{C_{1j}^E, C_{2j}^E\}$ and λ_{2j} are given in Appendix B.

3. The derivation of the integral equations

Define the dislocation functions as

$$\Delta u_r(r)=u_r(r,0)-u_r^E(r,0),\quad (0\le r<a) \tag{7a}$$

$$\Delta u_z(r)=u_z(r,0)-u_z^E(r,0),\quad (0\le r<a) \tag{7b}$$

Substitute Eqs. (4)-(6) into boundary conditions Eq. (1) and using Eq. (7), one obtains

$$\int_0^\infty\int_0^a \rho s\mathbf{J}_{10}(\rho r)\mathbf{P}(\rho)\mathbf{J}_{10}(\rho s)\mathbf{V}(s)dsd\rho=\mathbf{\Gamma}(r) \tag{8}$$

where

$$\mathbf{J}_{10}(\rho r)=diag\left[J_1(\rho r), J_0(\rho r)\right] \tag{9a}$$

$$\mathbf{\Gamma}(r)=\{l_1(r)\ \ l_2(r)\}^T=\int_0^\infty\int_0^a \rho s\mathbf{J}_{10}(\rho r)\boldsymbol{\gamma}(\rho)\tilde{\mathbf{J}}_{10}(\rho s)\mathbf{\Xi}(s)dsd\rho \tag{9b}$$

$$\mathbf{\Xi}(s)=\left\{p_1(s)\quad p_2(s)\quad p_3(s)\right\}^{\mathrm{T}} \tag{9c}$$

$$\tilde{\mathbf{J}}_{10}(\rho r)=diag[J_1(\rho r), J_0(\rho r), J_0(\rho r)] \tag{9d}$$

$$\mathbf{V}(s)=\left\{\Delta u_r(s)\quad \Delta u_z(s)\right\}^{\mathrm{T}} \tag{9e}$$

with $\mathbf{P}(\rho)$ and $\Upsilon(\rho)$ being given in Appendix C.

A set of new unknown functions are now introduced

$$d_1(r)=\frac{1}{r}\frac{\partial}{\partial r}\left\{ru_r(r,0)-ru_r^E(r,0)\right\} \tag{10a}$$

$$d_2(r) = \frac{\partial}{\partial r}\left\{u_z(r,0) - u_z^E(r,0)\right\} \tag{10b}$$

For the penny-shaped crack shown in Fig. 1, physical considerations require that

$$\left\{u_r(r,0) - u_r^E(r,0)\right\} \to 0\text{ , for } r \to a \tag{11a}$$

$$\left\{u_z(r,0) - u_z^E(r,0)\right\} \to 0\text{ , for } r \to a \tag{11b}$$

$$u_r(r,0) \to 0, \quad u_r^E(r,0) \to 0\text{, for } r \to 0 \tag{11c}$$

$$\frac{\partial}{\partial r}\left\{u_z(r,0) - u_z^E(r,0)\right\} \to 0\text{ , for } r \to 0 \tag{11d}$$

Therefore, the unknown function defined by Eq. (10) must satisfy the following conditions

$$\int_0^a r d_1(r)\, dr = 0 \tag{12a}$$

$$\int_0^a d_2(r)\, dr = 0 \tag{12b}$$

By partial integration of Eq. (8) and using Eq. (10), one can easily obtain

$$\int_0^\infty \int_0^a \rho s \mathbf{J}_{10}(\rho r)\mathbf{K}(\rho)\mathbf{J}_{01}(\rho s)\mathbf{F}(s)\, ds d\rho = \mathbf{\Gamma}(r) \tag{13}$$

where

$$\mathbf{J}_{01}(\rho s) = diag\left[J_0(\rho s), J_1(\rho s)\right] \tag{14a}$$

$$\mathbf{K}(\rho) = \frac{1}{\rho}\begin{bmatrix} P_{11}(\rho) & -P_{12}(\rho) \\ P_{21}(\rho) & -P_{22}(\rho) \end{bmatrix} \tag{14b}$$

$$\mathbf{F}(s) = \left\{d_1(s) \quad d_2(s)\right\}^{\mathrm{T}} \tag{14c}$$

In order to avoid divergent integrals, Eq. (13) is now integrated with respect to r to yield the following equation.

$$\int_0^\infty \int_0^a s\tilde{\mathbf{J}}_{01}(\rho r)\mathbf{K}(\rho)\mathbf{J}_{01}(\rho s)\mathbf{F}(s)\, d\rho ds = \tilde{\mathbf{\Gamma}}(r) \tag{15}$$

where

$$\tilde{\mathbf{J}}_{01}(\rho r) = diag[-J_0(\rho r), J_1(\rho r)] \tag{16a}$$

$$\tilde{\mathbf{\Gamma}}(r) = \left\{\int_0^r l_1(\zeta)d\zeta + C_1 \quad \frac{1}{\zeta}\left(\int_0^r \zeta l_2(\zeta)d\zeta + C_2\right)\right\}^T \tag{16b}$$

and C_1 and C_2 are integral constants.

After changing the order of integration, Eq. (15) can be written as

$$\int_0^a \int_0^\infty s\tilde{\mathbf{J}}_{01}(\rho r)\mathbf{M}\mathbf{J}_{01}(\rho s)\mathbf{F}(s)d\rho ds + \int_0^a \int_0^\infty s\tilde{\mathbf{J}}_{01}(\rho r)[\mathbf{K}(\rho)-\mathbf{M}]\mathbf{J}_{01}(\rho s)\mathbf{F}(s)d\rho ds = \tilde{\mathbf{\Gamma}}(r) \quad (17)$$

where

$$\mathbf{M} = \lim_{\rho\to\infty}\mathbf{K}(\rho) \quad (18)$$

Eq. (17) can be further expressed as

$$\int_0^a \sum \mathbf{F}(s) s ds + \int_0^a \int_0^\infty s\tilde{\mathbf{J}}_{01}(\rho r)[\mathbf{K}(\rho)-\mathbf{M}]\mathbf{J}_{01}(\rho s)\mathbf{F}(s)d\rho ds = \tilde{\mathbf{\Gamma}}(r) \quad (19)$$

where

$$\Sigma = \begin{bmatrix} -h_{11}M_{11} & -h_{12}M_{12} \\ h_{21}M_{21} & h_{22}M_{22} \end{bmatrix} \quad (20)$$

with

$$h_{11} = \int_0^\infty J_0(r\rho)J_0(s\rho)d\rho = \frac{2}{\pi}\begin{cases} \frac{1}{r}K(s/r), & s<r \\ \frac{1}{s}K(r/s), & s>r \end{cases} \quad (21a)$$

$$h_{22} = \int_0^\infty J_1(r\rho)J_1(s\rho)d\rho = \frac{2}{\pi}\begin{cases} \frac{1}{s}\left[K(s/r)-E(s/r)\right], & s<r \\ \frac{1}{r}\left[K(r/s)-E(r/s)\right], & s>r \end{cases} \quad (21b)$$

$$h_{12} = \int_0^\infty J_0(r\rho)J_1(s\rho)d\rho = \begin{cases} 0, & s<r \\ \frac{1}{s}, & s>r \end{cases} \quad (21c)$$

$$h_{21} = \int_0^\infty J_1(r\rho)J_0(s\rho)d\rho = \begin{cases} \frac{1}{r}, & s<r \\ 0, & s>r \end{cases} \quad (21d)$$

In Eqs. (21a) and (21b), $K(k)$ and $E(k)$ are, respectively, the complete elliptic integrals of the first and second kind, i.e.

$$K(k) = \int_0^{\pi/2} \frac{d\theta}{\sqrt{1-k^2\sin^2\theta}} \quad (22a)$$

$$E(k) = \int_0^{\pi/2} \sqrt{1-k^2\sin^2\theta}\, d\theta \quad (22b)$$

Differentiating Eq. (19) with respect to r yields

$$\mathbf{AF}(r)+\frac{1}{\pi}\int_0^a \frac{1}{s-r}\mathbf{BF}(s)ds+\int_0^a \mathbf{QF}(s)ds=\mathbf{\Gamma}(r) \tag{23}$$

where

$$\mathbf{A}=\begin{bmatrix} 0 & -M_{12} \\ M_{21} & 0 \end{bmatrix} \tag{24a}$$

$$\mathbf{B}=\begin{bmatrix} M_{11} & 0 \\ 0 & M_{22} \end{bmatrix} \tag{24b}$$

$$\mathbf{Q}=\boldsymbol{\kappa}\mathbf{B}+\int_0^\infty \rho s\mathbf{J}_{10}(\rho r)\left[\mathbf{K}(\rho)-\mathbf{M}\right]\mathbf{J}_{01}(\rho s)d\rho \tag{24c}$$

with

$$\boldsymbol{\kappa}=diag\left[\kappa_{11}(r,s),\kappa_{22}(r,s)\right] \tag{25a}$$

$$\kappa_{11}(r,s)=\frac{1}{\pi}\left[\frac{2rM_1(r,s)}{s^2-r^2}-\frac{1}{s-r}\right] \tag{25b}$$

$$\kappa_{22}(r,s)=\frac{1}{\pi}\left[\frac{2sM_2(r,s)}{s^2-r^2}-\frac{1}{s-r}\right] \tag{25c}$$

and

$$M_1(r,s)=\begin{cases} \dfrac{s}{r}E(s/r), & s<r \\ \dfrac{s^2}{r^2}E(r/s)-\dfrac{s^2-r^2}{r^2}K(r/s), & s>r \end{cases} \tag{26a}$$

$$M_2(r,s)=\begin{cases} \dfrac{r}{s}E(s/r)+\dfrac{s^2-r^2}{rs}K(s/r), & s<r \\ E(r/s), & s>r \end{cases} \tag{26b}$$

Introducing two non-dimensional variables η and ξ

$$s=a\eta/2+a/2 \tag{27a}$$

$$r=a\xi/2+a/2 \tag{27b}$$

Eq. (23) becomes

$$\mathbf{A\bar{F}}(\xi)+\frac{1}{\pi}\int_{-1}^1 \mathbf{B}\frac{\mathbf{\bar{F}}(\eta)}{\eta-\xi}d\eta+\int_{-1}^1 \mathbf{\bar{Q}}(\xi,\eta)\mathbf{\bar{F}}(\eta)d\eta=\mathbf{L}(\xi) \tag{28}$$

where

$$\bar{\mathbf{F}}(\eta)=\mathbf{F}\left(\frac{a}{2}\eta+\frac{a}{2}\right) \tag{29a}$$

$$\bar{\mathbf{Q}}(\eta,\xi)=\frac{a}{2}\mathbf{Q}\left(\frac{a}{2}\eta+\frac{a}{2},\frac{a}{2}\xi+\frac{a}{2}\right) \tag{29b}$$

$$\mathbf{L}(\xi)=\Gamma\left(\frac{a}{2}\xi+\frac{a}{2}\right) \tag{29c}$$

4. The solution of integral equations

To solve the Cauchy singular integral equation of the second type, an approximate method described in Shen and Kuang (1998) is employed.

Multiplying Eq. (28) by $\mathbf{B}^{-1}$ leads to

$$\mathbf{B}^{-1}\mathbf{A}\bar{\mathbf{F}}(\xi)+\frac{1}{\pi}\int_{-1}^{1}\frac{\bar{\mathbf{F}}(\eta)}{\eta-\xi}d\eta+\int_{-1}^{1}\mathbf{B}^{-1}\bar{\mathbf{Q}}(\xi,\eta)\bar{\mathbf{F}}(\eta)d\eta=\mathbf{B}^{-1}\mathbf{L}(\xi) \tag{30}$$

There exists a matrix $\mathbf{R}$ which is composed of eigenvectors of $\mathbf{B}^{-1}\mathbf{A}$ to make $\mathbf{B}^{-1}\mathbf{A}$ diagonal, i.e.

$$\mathbf{R}^{-1}\mathbf{B}^{-1}\mathbf{A}\mathbf{R}=\boldsymbol{\Lambda} \tag{31}$$

where $\boldsymbol{\Lambda}$ is the diagonal matrix of eigenvalues. Eq. (30) can be further expressed as

$$\boldsymbol{\Lambda}\mathbf{G}(\xi)+\frac{1}{\pi}\int_{-1}^{1}\frac{\mathbf{G}(\eta)}{\eta-\xi}d\eta+\int_{-1}^{1}\boldsymbol{\Theta}(\eta,\xi)\mathbf{G}(\eta)d\eta=\bar{\mathbf{L}}(\xi) \tag{32}$$

where

$$\mathbf{G}(\eta)=\mathbf{R}^{-1}\bar{\mathbf{F}}(\eta) \tag{33a}$$

$$\boldsymbol{\Theta}(\eta,\xi)=\mathbf{R}^{-1}\mathbf{B}^{-1}\bar{\mathbf{Q}}(\eta,\xi)\mathbf{R} \tag{33b}$$

$$\bar{\mathbf{L}}(\xi)=\mathbf{R}^{-1}\mathbf{B}^{-1}\mathbf{L}(\xi) \tag{33c}$$

The solutions of Eq. (32) can be expressed in the form

$$\mathbf{G}(\xi)=diag\left[W_1(\xi)\quad W_2(\xi)\right]\begin{Bmatrix}\sum_{s=0}^{\infty}A_s P_s^{(\alpha_1,\beta_1)}(\xi)\\ \sum_{s=0}^{\infty}B_s P_s^{(\alpha_2,\beta_2)}(\xi)\end{Bmatrix} \tag{34}$$

where $P_s^{(\alpha_j,\beta_j)}\ (j=1,2)$ are the Jacobi polynomials, and $W_j(\xi)=(1-\xi)^{\alpha_j}(1+\xi)^{\beta_j}$ is the weight function of Jacobi polynomials with

$$\alpha_j=-\frac{1}{2}+\frac{\mathrm{i}}{2\pi}\ln\frac{1-\mathrm{i}\gamma_j}{1+\mathrm{i}\gamma_j},\quad \beta_j=\frac{1}{2}-\frac{\mathrm{i}}{2\pi}\ln\frac{1-\mathrm{i}\gamma_j}{1+\mathrm{i}\gamma_j} \tag{35}$$

where γ_j are the elements of the eigenvalue matrix $\mathbf{\Lambda}$. From Eqs. (34), (35) and constitutive equations, one knows that there is oscillating singularity of stress around the crack tip.

Substituting Eq. (34) into Eq. (32), one obtains the following system of algebraic equations

$$\sum_{s=0}^{N}\left[T_{ms}^{11}A_s+T_{ms}^{12}B_s\right]=L_m^1 \tag{36a}$$

$$\sum_{s=0}^{N}\left[T_{ms}^{21}A_s+T_{ms}^{22}B_s\right]=L_m^2 \tag{36b}$$

where

$$\begin{aligned}T_{ms}^{ij}&=\frac{\left(1+\gamma_i^2\right)^{1/2}}{2}\theta_{s-1}^{(-\alpha_i,-\beta_i)}\delta_{m(s-1)}\delta_{ij}\\&+\int_{-1}^{1}\int_{-1}^{1}W_{-i}(\xi)P_m^{(-\alpha_i,-\beta_i)}(\xi)\mathbf{\Theta}_{ij}(\eta,\xi)W_j(\eta)P_s^{(\alpha_j,\beta_j)}(\eta)d\eta d\xi\end{aligned} \tag{37a}$$

$$L_m^i=\int_{-1}^{1}W_{-i}(\xi)P_m^{(-\alpha_i,-\beta_i)}(\xi)\bar{\mathbf{L}}_i d\xi,\quad m=0,1,\cdots,N-1,\quad i,j=1,2 \tag{37b}$$

with

$$W_{-j}(\xi)=(1-\xi)^{-\alpha_j}(1+\xi)^{-\beta_j} \tag{37c}$$

$$\theta_k^{(\alpha,\beta)}=\frac{2^{(\alpha+\beta+1)}\Gamma(\alpha+k+1)\Gamma(\beta+k+1)}{k!(\alpha+\beta+2k+1)\Gamma(\alpha+\beta+k+1)} \tag{37d}$$

and δ_{ij} being the Kronecker Delta function.

Therefore, A_s and B_s can be obtained from Eq. (36) and the following equation yield from Eq. (12)

$$\int_{-1}^{1}diag\left\{\frac{a}{2}\eta+\frac{a}{2},1\right\}\mathbf{R}diag\{W_1(\eta),W_2(\eta)\}\left\{\sum_{s=0}^{N}A_sP_s^{(\alpha_1,\beta_1)}(\eta)\ \sum_{s=0}^{N}B_sP_s^{(\alpha_2,\beta_s)}(\eta)\right\}^T d\eta=0 \tag{38}$$

5. Field intensity factors and energy release rates

After the constants A_s and A_s (s=0,1,2,…N) have been determined from Eqs. (36) and (38), define the equivalent stress intensity factors (SIFs) including mode-I SIF and mode-II SIF, of the crack tip as

$$\mathbf{K}^e=\begin{Bmatrix}K_{\mathrm{II}}^e\\K_{\mathrm{I}}^e\end{Bmatrix}=\sqrt{a}\lim_{\xi\to1^+}\begin{bmatrix}(\xi-1)^{-\alpha_1}&0\\0&(\xi-1)^{-\alpha_2}\end{bmatrix}\left\{\mathbf{\Lambda}\mathbf{G}(\xi)+\frac{1}{\pi}\int_{-1}^{1}\frac{\mathbf{G}(\eta)}{\eta-\xi}d\eta+\int_{-1}^{1}\mathbf{\Theta}(\eta,\xi)\mathbf{G}(\eta)d\eta\right\} \tag{39}$$

It should be noted that the oscillating singularity of stress can be eliminated in the process of derivation of SIFs.

Then comparing the right-hand sides of Eqs. (30) and (32), one can obtain the relation between the actual SIFs and the equivalent SIFs as

$$\mathbf{K} = \mathbf{B}\mathbf{R}\mathbf{K}^{e} \tag{40}$$

Finally, the SIFs at the crack tip can be deduced as

$$\mathbf{K} = -\sqrt{a}\mathbf{B}\mathbf{R}\sum_{s=0}^{N}\begin{Bmatrix} \left(1+\gamma_1^2\right)^{1/2} 2^{\beta_1} P_s^{(\alpha_1,\beta_1)}(1) A_s \\ \left(1+\gamma_2^2\right)^{1/2} 2^{\beta_2} P_s^{(\alpha_2,\beta_2)}(1) B_s \end{Bmatrix} \tag{41}$$

In accordance with the definition of the energy release rate (ERR), the ERR of the crack tip can be derived as

$$G = \frac{1}{4}\mathbf{K}^{e\mathrm{T}}\Pi\Omega\mathbf{K}^{e} \tag{42}$$

where

$$\Pi_{ij} = \left(\frac{a}{2}\right)^{-(1+\alpha_i+\alpha_j)} \frac{1}{1+\alpha_j} \mathrm{N}_{ij} \frac{\Gamma(1+\alpha_i)\Gamma(2+\alpha_j)}{\Gamma(3+\alpha_i+\alpha_j)} \tag{43a}$$

$$\Omega_{ij} = \left(1+\gamma_i^2\right)^{-1/2} \delta_{ij} \tag{43b}$$

with

$$\mathbf{N} = \mathbf{R}^{\mathrm{T}}\mathbf{B}^{\mathrm{T}}\mathbf{R} \tag{43c}$$

6. Numerical results

For the numerical examples, the PZT-5H is considered as the piezoelectric layer. The material properties of which are given as follows

$c_{11} = 126\text{GPa},\ c_{13} = 53\text{GPa},\ c_{33} = 117\text{GPa},\ c_{44} = 35.3\text{GPa},\ e_{31} = -6.5\text{C/m}^2,$

$e_{33} = 23.3\text{C/m}^2,\ e_{15} = 17.0\text{C/m}^2,\ \varepsilon_{11} = 15.1\times10^{-9}\,\text{C}^2/(\text{Nm}^2),\ \varepsilon_{33} = 13.0\times10^{-9}\,\text{C}^2/(\text{Nm}^2).$

The material properties of the elastic half-space can be set as

$$c_{11}^{E} = r_1 c_{11},\ c_{13}^{E} = r_2 c_{13},\ c_{33}^{E} = r_3 c_{33},\ c_{44}^{E} = r_4 c_{44}. \tag{44}$$

For simplicity, only the loading case of $\Gamma(r)=\{0\ \sigma_0\ D_0\}^{\mathrm{T}}$ is considered. Also, D_0 is determined by the load combination parameters $\lambda_D=D_0c_{33}/(\sigma_0 e_{33})$. The numerical results are plotted in Figs. 2-9, where the mode-I SIF K_I and mode-II SIF K_{II} are normalized by K_0 with

$$K_0 = \sigma_0 a^{1/2} \tag{45}$$

And the energy release rates G is normalized by G_0, which can be expressed as

$$G_0 = \frac{\pi}{4} \bar{B}_{22} \sigma_0^2 a \tag{46}$$

where $\bar{B}_{22}$ is the element of matrix $\bar{\mathbf{B}}$, with

$$\bar{\mathbf{B}} = \mathbf{B}^{-1} \tag{47}$$

Accuracy of the present formulation is first verified by comparing with analytical solution reported for a penny-shaped crack in an ideal elastic material. In the present problem, the piezoelectric layer with the same elastic properties as elastic half-space is selected, but the piezoelectric and dielectric constants are set to negligibly small values. The normalized modes I and II SIFs under purely mechanical loading are shown in Fig. 2. It is clear that with the increasing of *h/a*, the normalized mode-I and II SIF approaches to $2/\pi$ and zero corresponding to the asymptotic value of a penny-shaped crack in an infinite homogeneous elastic material (Kassir and Sih 1975). The normalized ERR is plotted in Fig. 3. Normalized ERR approaches to $4/\pi^2$ with the increasing of *h/a*.

The effect of electric loading on normalized ERRs of the crack tips is plotted in Fig. 4. Fig. 4 shows that the normalized ERRs increase linearly with the increasing of λ_D for a smaller *h/a*. With the increasing of *h/a*, the effect of electric loading on the SIF becomes increasingly weak. This means that increasing electric loading is liable to promote the crack extension.

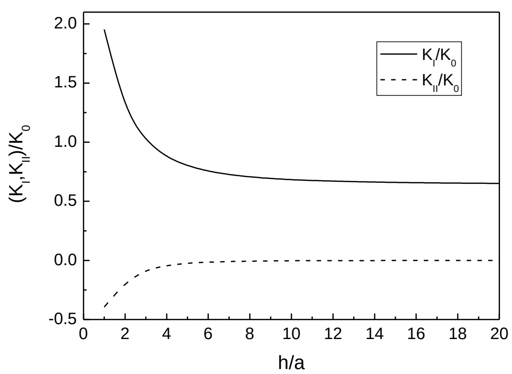

Fig. 2 Variations of normalized mode I and II SIFs with *h/a*

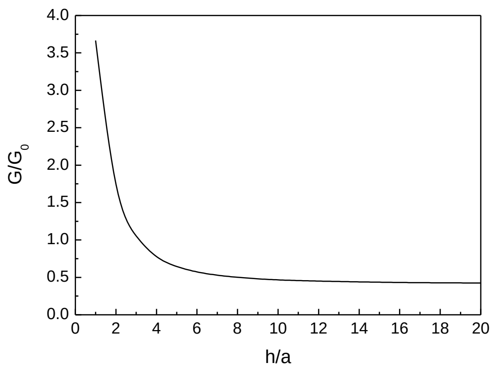

Fig. 3 Variations of normalized ERR with *h/a*

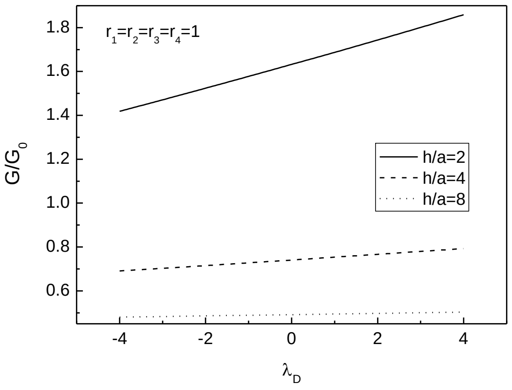

Fig. 4 Variations of normalized ERR with λ_D under different *h/a*

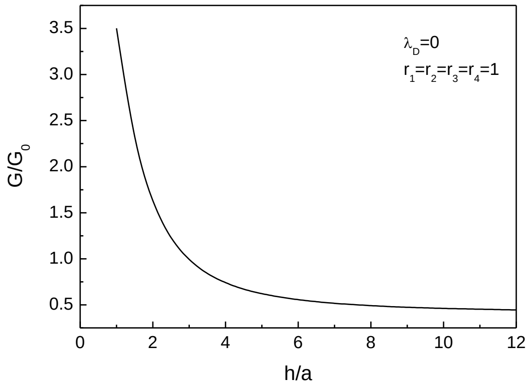

Fig. 5 Variations of normalized ERR with *h/a* (r_1=r_2=r_3=r_4=1)

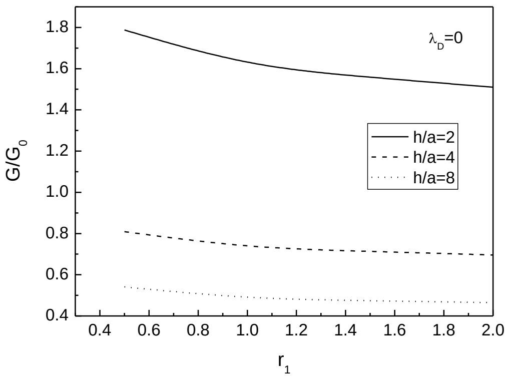

Fig. 6 Variations of normalized ERR with r_1 under λ_D=0 and different *h/a*

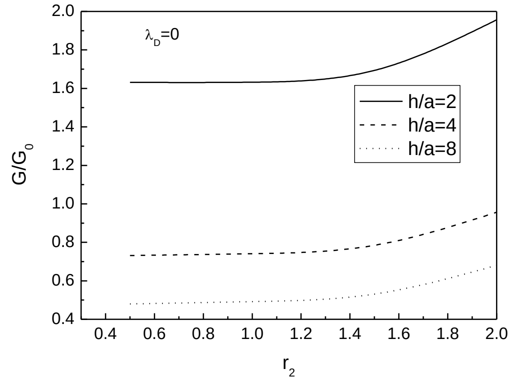

Fig. 7 Variations of normalized ERR with r_2 under λ_D=0 and different *h/a*

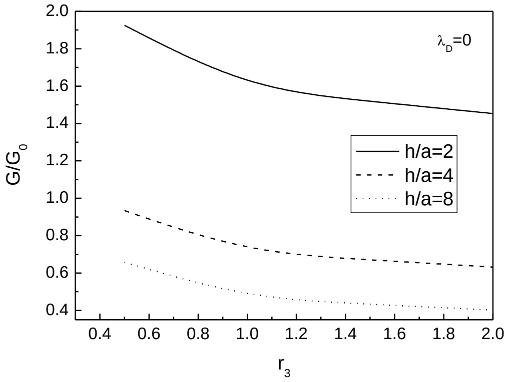

Fig. 8 Variations of normalized ERR with r_3 under λ_D=0 and different *h/a*

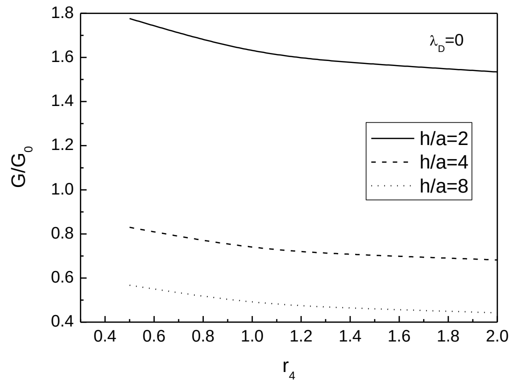

Fig. 9 Variations of normalized ERR with r_4 under λ_D=0 and different *h/a*

Fig. 5 show the effect of the *h/a* on the normalized ERR. As expected, the ERR decrease with increasing *h/a*. Therefore, increasing the thickness of the layer can suppress the crack extension.

The effects of material combination on the ERR can be seen from Figs. 6-9. It is found that different components of the elastic moduli tensor different by influence the ERR. As shown in Fig. 6 and Figs. 8-9, the normalized ERRs decrease with the increasing of r_1, r_3 and r_4. However, as the value of r_2 increases, the normalized ERR increases (Fig. 7). This means that increasing c_{11}, c_{33} and c_{44} or decreasing c_{13} of elastic half-space will be benefit for the stable of the structure.

7. Conclusions

In this paper, the interfacial penny-shaped crack between piezoelectric layer and elastic half-space under mechanical and electric loadings is investigated. Hankel transforms and dislocation density functions are used to reduce the mixed boundary value problem to a system of Cauchy singular equations. With the aid of Jacobi polynomials the integral equations are further reduced to a system of algebraic equations, which can be numerically solved. According to energy release rate fracture criterion, the following conclusions may be drawn:

(i) Decreasing the electric loading can suppress the crack propagation or growth.

(ii) Increasing c_{11}, c_{33} and c_{44} or decreasing c_{13} of elastic half-space will be benefit for the stable of the structure.

(iii) Increasing the thickness of the piezoelectric layer will be beneficial to remain the crack stable.

Acknowledgments

The research described in this paper was financially supported by the Natural Science Foundation of Hebei Province, China (E2013402077), the Natural Science Foundation of China (11272223) and the Program for Leading Talent of Innovative Research Team of University in Hebei Province, China.

References

Chen, W.Q. and Shioya, T. (2000), "Complete and exact solutions of a penny-shaped crack in a piezoelectric solid: antisymmetric shear loadings", *Int. J. Solids Struct.*, **37**, 2603-2619.

Feng, W.J., Li, Y.S. and Ren, D.L. (2006), "Transient response of a piezoelectric layer with a penny-shaped crack under electrical-mechanical impacts", *Struct. Eng. Mech.*, **23**, 163-176.

Karapetian, E., Sevotianov, I. and Kachanov, M. (2000), "Penny-shaped and half-plane cracks in a transversely isotropic piezoelectric solid under arbitrary loading", *Arch. Appl. Mech.*, **70**, 201-229.

Kassir, M.K. and Sih, G.C. (1975), *Three-Dimensional Crack Problems*, Noordhoff International Publications, Leyden.

Kogan, L., Hui, C.Y. and Molkov, V. (1996), "Stress and induction field of a spherical inclusion or a penny-shaped crack in a transversely isotropic piezoelectric material", *Int. J. Solids Struct.*, **33**, 2719-2737.

Kuna, M. (2010), "Fracture mechanics of piezoelectric materials-where are we right now?", *Eng. Fract. Mech.*, **77**, 309-326.

Li, X.F. and Lee, K.Y. (2004), “Effects of electric field on crack growth for a penny-shaped dielectric crack in a piezoelectric layer”, *J. Mech. Phys. Solid.*, **52**, 2079-2100.

Shang, F., Kuna, M. and Abendroth, M. (2003), “Finite element analyses of three-dimensional crack problems in piezoelectric structures”, *Eng. Fract. Mech.*, **70**, 143-160.

Shen, S.P. and Kuang, Z.B. (1998), “Wave scattering from an interface crack in laminated anisotropic media”, *Mech. Res. Commun.*, **25**, 509-517.

Tian, W.Y. and Rajapakse, R.K.N.D. (2006), “Fracture parameters of a penny-shaped crack at the interface of a piezoelectric bi-material system”, *Int. J. Fract.*, **141**, 37-48.

Ueda, S. (2008), “Functionally graded piezoelectric strip with a penny-shaped crack under electromechanical loadings”, *Eur. J. Mech. A/Solid*., **27,** 50-60.

Ueda, S. and Ashida, F. (2007), “Transient response of a functionally graded piezoelectric strip with a penny-shaped crack under electric time-dependent loading”, *Acta Mech*., **194**, 175-190.

Wang, B.L., Noda N., Han, J.C. and Du, S.Y. (2001), “A penny-shaped crack in a transversely isotropic piezoelectric layer”, *Eur. J. Mech. A/Solid*, **20**, 997-1005.

Wang, B.L., Sun, Y.G. and Zhu, Y. (2011), “Fracture of a finite piezoelectric layer with a penny-shaped crack”, *Int. J. Fract.*, **172**, 19-39.

Wang, Z.K. (1994), “Penny-shaped crack in transversely isotropic piezoelectric materials”, *Acta. Mech. Sin.*, **10**, 49-60.

Yang, F.Q. (2004), “General solutions of a penny-shaped crack in a piezoelectric material under opening mode-I loading”, *Q. J. Mech. Appl. Math*., **57**, 529-550.

Yang, J.H. and Lee, K.Y. (2003a), “Penny-shaped crack in a piezoelectric cylinder under electromechanical loads”, *Arch. Appl. Mech.*, **73**, 323-336.

Yang, J.H. and Lee, K.Y. (2003b), “Penny-shaped crack in a piezoelectric cylinder surrounded by an elastic medium subjected to combined in plane mechanical and electrical loads”, *Int. J. Solids Struct.*, **40**, 573-590.

Zhang, T.Y. and Gao, C.F. (2004), “Fracture behaviors of piezoelectric materials”, *Theor. Appl. Fract. Mech.*, **41**, 339-379.

Zhang, T.Y., Zhao, M.H. and Tong, P. (2002), “Fracture of piezoelectric ceramics”, *Adv. Appl. Mech.*, **38**, 147-289.

Appendix A

The constants $\{a_{1j}, a_{2j}, a_{3j}\}$ and parameters λ_{1j} are satisfy

$$\begin{bmatrix} c_{11}-c_{44}\lambda_{1j}^2 & (c_{13}+c_{44})\lambda_{1j} & (e_{31}+e_{15})\lambda_{1j} \\ (c_{13}+c_{44})\lambda_{1j} & c_{33}\lambda_{1j}^2-c_{44} & e_{33}\lambda_{1j}^2-e_{15} \\ (e_{31}+e_{15})\lambda_{1j} & e_{33}\lambda_{1j}^2-e_{15} & \varepsilon_{11}-\varepsilon_{33}\lambda_{1j}^2 \end{bmatrix} \begin{Bmatrix} a_{1j} \\ a_{2j} \\ a_{3j} \end{Bmatrix} = 0 \tag{A1}$$

and

$$C_{1j} = c_{44}\lambda_{1j}a_{1j} - c_{44}a_{2j} - e_{15}a_{3j} \tag{A2}$$

$$C_{2j} = c_{13}a_{1j} + c_{33}\lambda_{1j}a_{2j} + e_{33}\lambda_{1j}a_{3j} \tag{A3}$$

$$C_{3j} = e_{31}a_{1j} + e_{33}\lambda_{1j}a_{2j} - \varepsilon_{33}\lambda_{1j}a_{3j} \tag{A4}$$

Appendix B

The constants $\{a_{1j}^E, a_{2j}^E\}$ and parameters λ_{2j} are satisfy

$$\begin{bmatrix} c_{11}^E-c_{44}^E\lambda_{2j}^2 & (c_{13}^E+c_{44}^E)\lambda_{2j} \\ (c_{13}^E+c_{44}^E)\lambda_{2j} & c_{33}^E\lambda_{2j}^2-c_{44}^E \end{bmatrix} \begin{Bmatrix} a_{1j}^E \\ a_{2j}^E \end{Bmatrix} = 0 \tag{B1}$$

where λ_{2j} are two pairs of complex conjugate. $\text{Real}(\lambda_{2j}) > 0$ and corresponding characteristic vector are selected here. And C_{1j}^E and C_{2j}^E are

$$C_{1j}^E = c_{44}^E\lambda_{2j}a_{1j}^E - c_{44}^E a_{2j}^E \tag{B2}$$

$$C_{2j}^E = c_{13}^E a_{1j}^E + c_{33}^E\lambda_{2j}a_{2j}^E \tag{B3}$$

Appendix C

Matrix $\mathbf{P}(\rho)$ and $\Upsilon(\rho)$ are

$$\mathbf{P}(\rho) = \begin{bmatrix} \sum_{j=1}^{6} \frac{H_{1j}\Delta_{4j}(\rho)}{\Delta(\rho)} & \sum_{j=1}^{6} \frac{H_{1j}\Delta_{5j}(\rho)}{\Delta(\rho)} \\ \sum_{j=1}^{6} \frac{H_{2j}\Delta_{4j}(\rho)}{\Delta(\rho)} & \sum_{j=1}^{6} \frac{H_{2j}\Delta_{5j}(\rho)}{\Delta(\rho)} \end{bmatrix} \tag{C1}$$

$$\Upsilon(\rho)=\begin{bmatrix}\sum_{j=1}^{6}\frac{H_{1j}\Delta_{6j}(\rho)}{\Delta(\rho)} & \sum_{j=1}^{6}\frac{H_{1j}\Delta_{7j}(\rho)}{\Delta(\rho)} & \sum_{j=1}^{6}\frac{H_{1j}\Delta_{8j}(\rho)}{\Delta(\rho)} \\ \sum_{j=1}^{6}\frac{H_{2j}\Delta_{6j}(\rho)}{\Delta(\rho)} & \sum_{j=1}^{6}\frac{H_{2j}\Delta_{7j}(\rho)}{\Delta(\rho)} & \sum_{j=1}^{6}\frac{H_{2j}\Delta_{8j}(\rho)}{\Delta(\rho)}\end{bmatrix} \tag{C2}$$

where $\Delta(\rho)$ is the determinant of the coefficient matrix $\mathbf{H}$, whose elements can be expressed as H_{ij} with ith row and jth column; $\Delta_{kj}(\rho)$ (k=4,5,…8) are, respectively, the corresponding algebra cofactors.

$$H_{1j}=C_{1j},\quad H_{1k}=C_{1j}^{E}$$
$$H_{2j}=C_{2j},\quad H_{2k}=C_{2j}^{E}$$
$$H_{3j}=C_{3j},\quad H_{3k}=0$$
$$H_{4j}=a_{1j}/\rho,\quad H_{4k}=a_{1j}^{E}/\rho$$
$$H_{5j}=b_{2j}/\rho,\quad H_{5k}=b_{2j}^{E}/\rho$$
$$H_{6j}=C_{1j}\exp\left(\rho\lambda_{1j}h\right),\quad H_{6k}=0$$
$$H_{7j}=C_{2j}\exp\left(\rho\lambda_{1j}h\right),\quad H_{7k}=0$$
$$H_{8j}=C_{3j}\exp\left(\rho\lambda_{1j}h\right),\quad H_{8k}=0$$

where j=1,2,…,6, k=1,2.